Vanadia supported on ceria: Characterization and activity in liquid-phase oxidation of ethylbenzene

T. Radhika, S. Sugunan *

Department of Applied Chemistry, Cochin University of Science and Technology, Cochin-22, Kerala 682022, India

Abstract

Vanadia/ceria catalysts (2–10 wt% of V_2O_5) were prepared by wet impregnation of ammonium metavanadate in oxalic acid solution. Structural characterization was done with energy dispersive X-ray analysis (EDX), powder X-ray diffraction (XRD), BET surface area measurements, FT-IR spectroscopy and nuclear magnetic spectral analysis (^{51}V MASNMR). XRD and ^{51}V MASNMR results show highly dispersed vanadia species at lower loadings and the formation of $CeVO_4$ phase at higher V_2O_5 loading. The catalytic activity of catalysts was conducted in liquid phase oxidation of ethylbenzene with H_2O_2 as oxidant. The oxidation activity is increased with loading up to 8 wt% V_2O_5 and then decreased with further increase in V_2O_5 content to 10 wt%. Different vanadia species evidenced by various techniques were found to be selective towards ethylbenzene oxidation. The $CeVO_4$ formation associated with increased concentration of vanadia on ceria results the production of acetophenone along with 2-hydroxyacetophenone.
© 2006 Elsevier B.V. All rights reserved.

Keywords: Vanadia; Ceria; $CeVO_4$; Ethylbenzene oxidation; ^{51}V MASNMR

1. Introduction

Supported vanadium oxide catalysts have been extensively used for catalyzing several oxidation reactions [1–5]. The redox chemistry of ceria is a critical parameter in the efficiency of multifunctional components of three-way automotive catalysts and applications of these materials in various other catalytic processes such as oxygen permeation membrane systems, deNO$_x$ catalysis, oxidation of aromatics and catalytic wet oxidation are being extensively studied [6,7]. In recent years vanadia/ceria combination catalysts have been the subjects of numerous investigations because of its wide range applications in catalysis and material science [8,9]. Generally, oxidation rate is limited by the oxygen transfer from the liquid phase to the metal oxide sites, while ceria is able to enhance this oxygen transfer to efficiently catalyze the reactions. The redox proper-

ties of ceria (Ce^{4+}/Ce^{3+}) and the high lability of its lattice oxygen are among the most important factors that contribute to the catalytic reactivity in oxidation reactions [10].

Side-chain oxidation of alkyl aromatics using cleaner peroxide oxidants catalyzed by heterogeneous catalysts has been much interesting [11]. Effective utilization of ethylbenzene, available in the xylene stream of the petrochemical industry to more value added products is a promising one in chemical industry. The oxidation products of ethylbenzene are widely employed as intermediates in organic, steroid and resin synthesis [12–14]. Zeolite encapsulated Co(II), Ni(II) and Cu(II) complexes gave acetophenone as the only partial oxidation product during ethylbenzene oxidation with H_2O_2 [15]. Titanosilicates mainly catalyze ring hydroxylation of arenes with H_2O_2, whereas vanadium and chromium substituted zeolites and aluminophosphate molecular sieves have been known to favour side-chain oxidation selectively [16].

In the present work, we report the structural characterization of ceria supported vanadia catalysts for various loading of V_2O_5 observed using different physico-chemical

* Corresponding author. Tel.: +91 484 2575804; fax: +91 484 2577595.
E-mail address: ssg@cusat.ac.in (S. Sugunan).

techniques. Activity of the catalysts towards liquid phase oxidation of ethylbenzene is also investigated and correlated with different vanadia species on the supported catalysts. The observed effect of reaction parameters such as temperature, solvent, substrate and oxidant concentration, catalyst weight and time have also been described.

2. Experimental

2.1. Catalyst preparation

Ceria was prepared by precipitation of hydroxide from 0.05 M $Ce(NO_3)_3 \cdot 6H_2O$ (Indian Rare Earth Ltd., Udyogamandal, Kerala) with 1:1 ammonia solution at pH 10.3. Vanadia/ceria catalysts were prepared by wet impregnation. To impregnate vanadia with loadings of 2, 4, 6, 8 and 10 (wt% V_2O_5), the requisite quantity of NH_4VO_3 (CDH, LR) was dissolved (0.001 M) in aqueous oxalic acid solution (0.1 M) and to this dried ceria was added and mechanically stirred for 6 h. After keeping it overnight, the excess water was evaporated and the resulting material was oven dried at 383 K for 12 h and sieved to mesh size below 100 μm. All the catalysts were calcined at 773 K for 5 h in a closed muffle furnace in flowing air prior to use. Prepared catalysts are denoted as xVC, where x = 2, 4, 6, 8 and 10 wt% V_2O_5 and VC for V_2O_5/CeO_2.

2.2. Characterization

The chemical compositions of catalysts were obtained from Stereoscan 440 Cambridge, UK energy dispersive X-ray analyzer. XRD pattern was collected on Rigaku D-Max Ni filtered Cu Kα radiation. BET surface area and total pore volume were obtained using N_2 adsorption method at 77 K on Micromeritics Flow Prep-060 Gemini 2360 instrument. Infrared spectra were recorded with KBr pellets on an ABB BOMEM (MB Series) FT-IR spectrometer model in the range 400–4000 cm^{-1}. Solid-state ^{51}V MASNMR experiments of catalysts calcined at 773 K were carried out over a Bruker DSX-300 spectrometer with a standard 4 mm double bearing Bruker MAS probe (spinning frequency v_p = 7.0 kHz). Isotropic chemical shifts are reported relative to neat NH_4VO_3 (δiso = −570.4 ppm) as the reference.

2.3. Oxidation of ethylbenzene

The liquid-phase oxidation of ethylbenzene was carried out in a 50 mL round bottom flask. The flask was immersed in an oil bath in order to make the working temperature constant, which was connected with a condenser. In a typical run, catalyst and substrate were added to the solvent. The oxidant, 30% H_2O_2 was added to the system after attaining the reaction temperature. The reaction mixture was stirred using a magnetic stirrer. Reaction products were analyzed on Chemito 1000 GC equipped with FID detector and a BP-1 capillary column. Analysis was done

using a linear temperature programme (333 K–3 K 293 K/min–553 K) with injection and detection pot temperatures as 523 K. The products obtained were identified by comparison with standard ones. The catalytic activity was expressed as the percentage conversion (wt%) of ethylbenzene and the selectivity for a product is expressed as the amount of the particular product divided by total amount of products multiplied by 100.

3. Results and discussion

3.1. Physico-chemical characterization

The elemental composition as atom % of catalysts is presented in Table 1. The results indicate that effective loading of vanadium took place on ceria. The powder XRD pattern of VC catalysts along with that of CeO_2 and V_2O_5 collected after calcination at 773 K are presented in Fig. 1. The X-ray reflections of CeO_2 show a typical cubic crystal structure of fluorite type [17]. The diffraction pattern of VC series of catalysts show lines due to ceria along with additional peaks at higher loadings. Lines of $CeVO_4$ are observed as the loading increases with absence of any characteristic lines due to V_2O_5 [18]. This indicates that vanadia is finely dispersed on the ceria surface for 2, 4 and 6 wt%

Table 1
Chemical composition and physical properties of catalysts

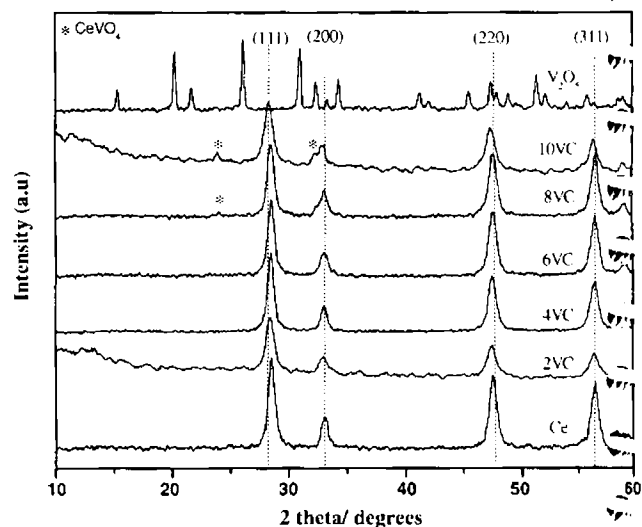| Catalyst	Composition (atom %)		BET surface area (m^2 g^{-1})	Pore volume (cm^3 g^{-1})	Crystallite size (nm)
	Ce	V			
Ce	100.00		67	0.11	12
2VC	93.23	6.77	64	0.10	9
4VC	90.44	9.56	36	0.06	19
6VC	89.60	10.40	46	0.11	13
8VC	86.84	13.16	49	0.05	15
10VC	83.47	16.53	44	0.03	10

Fig. 1. Powder XRD pattern of CeO_2, VC catalysts and V_2O_5.

V_2O_5 loading. For loading above 6 wt%, in addition to sharp ceria lines, new lines with less intensity can be seen at $2\theta/° = 24.0$ and 32.5, respectively. These are attributed to the formation of the mixed phase $CeVO_4$ [19]. The intensity of these lines increased steadily with increasing the amount of supported vanadia content. It is possible that CeO_2 and V_2O_5 could react together in the solid state in the temperature range 773–1073 K to form $CeVO_4$ [21]. During the formation of $CeVO_4$, cerium is reduced from Ce^{4+} to Ce^{3+}, whereas the vanadium reactant remains in the 5+ oxidation state. The reduction of Ce^{4+} in preference to V^{5+} is occurred by the fact that cerium frequently exhibits a valence of 3+ [22].

The specific surface area and pore volumes of catalysts are presented in Table 1. A substantial decrease in BET surface area can be observed after impregnation of the support with V_2O_5. The observed decrease is mainly due to penetration of the dispersed vanadia into the pores of the support. Additionally, solid-state reactions between the dispersed vanadia and ceria may also contribute to the observed decrease due to the formation of orthovanadate crystals, which block the pores of the support [22]. The formation of $CeVO_4$ at relatively low temperature could be probably favoured by the preparation method, since V_2O_5 was impregnated on the support in the present study. Above a particular concentration, V_2O_5 can interact with the support material and form compounds or multilayer species [23,24]. The TGA/DTA of catalysts exhibit endotherms and exotherms associated with the removal of physisorbed water and decomposition of oxalate species formed during the impregnation of vanadia on the support (figure not shown) [25].

FT-IR spectra of representative catalysts are shown in Fig. 2. In the infrared region the absorption bands at 465 and 1384 cm⁻¹ are characteristics of ceria [26]. For VC catalysts the absorption bands are visible in the range 795–805 and 1000–1100 cm⁻¹ in addition to those observed for ceria. The band at 1022 cm⁻¹ was reported to the V=O stretching vibration, while that at 818 cm⁻¹ was attributed to the cou-

pled vibrations between V=O and V–O–V [27,28]. A band observed at 1024 cm⁻¹ for 2VC is corresponding to surface V=O stretching mode and at 801 cm⁻¹ due to coupled vibration [29]. The intensity of the V=O absorption is decreased and more intense band at 799 cm⁻¹ is observed with increasing vanadia to 10VC which arises from the VO_4^{3-} species of orthovanadate structure [30].

The solid-state ⁵¹V MASNMR spectra of catalysts recorded are shown in Fig. 3. Different types of signals are observed in the spectra with varying intensities depending
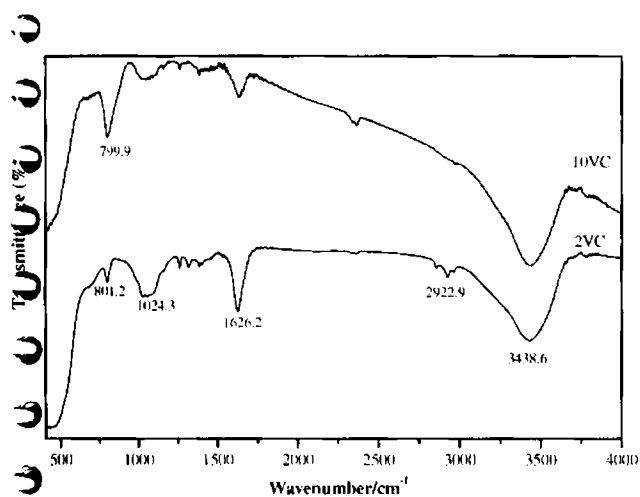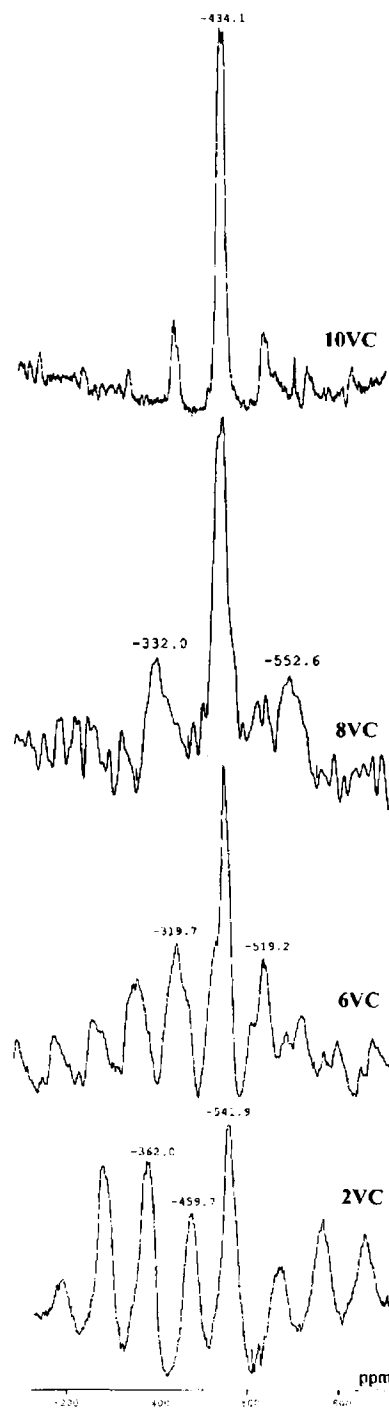

Fig. 2. FT-IR spectra of 2VC and 10VC.

Fig. 3. ⁵¹V MASNMR spectra of VC catalysts.

on the vanadia content. For 2VC, the peaks observed present a species characterized by isotropic component and several associated spinning bands. The broad line pattern associated with this species could be correlated with an absence of regular ordering of these vanadia sites. The peak at ~260 ppm is assigned to the surface vanadium–oxygen structures surrounded by a distorted octahedron of oxygen atoms [31]. The band at ~360 ppm can be assigned to pseudo-octahedrally coordinated V^{5+} species as a consequence of the interaction of tetrahedral sites. The resonances at ~459 and ~495 ppm can be attributed to distorted isolated tetrahedral V^{5+} sites. The peaks at ~545 and ~750 ppm are attributed to the tetrahedral vanadium–oxygen structures. Hence, in this low vanadia loaded catalysts, the species are consistent with surface V=O and polymeric species V–O–V, highly dispersed on the ceria surface [32]. For samples with higher vanadia loading (6VC, 8VC, 10VC) a highly symmetric signal centered at −432 ppm has been obtained. It has been reported that the signal with −432 ppm corresponds to the tetragonal structure of CeVO₄, in which vanadium atoms are located at the center of isolated tetrahedral [33]. The only peak of 10VC observed at −432 ppm due to the CeVO₄ implies that most of the V_2O_5 on the surface of ceria were consumed to form the CeVO₄ compound. These observations are in

good agreement with the results of XRD and Raman analysis.

The structural characterization of vanadia/ceria catalysts by various technique such as XRD, FT-IR, TGA, DTA and ^{51}V MASNMR show the presence of highly dispersed vanadia on lower loading of V_2O_5 and formation of CeVO₄ as the loading increases to 10 wt% V_2O_5. Low loading consists vanadia as tetrahedral V=O species while higher loading leads to the formation of Ce–O–V species on the ceria support surface.

3.2. Oxidation of ethylbenzene

The influence of different reaction parameters was analyzed in order to maximize the product yield and selectivity. Effect of reaction conditions for ethylbenzene oxidation with H_2O_2 was initially assayed in non-optimized conditions with 6VC as the catalyst.

The effect of temperature on the rate and selectivity of ethylbenzene oxidation is shown in Fig. 4(a). Oxidation of ethylbenzene using H_2O_2 in acetonitrile produced acetophenone as the major product. Benzaldehyde and 2-hydroxyacetophenone are also formed as oxidation products. Few temperatures have been tested and found that as the temperature rises, there is an increase in the oxidation
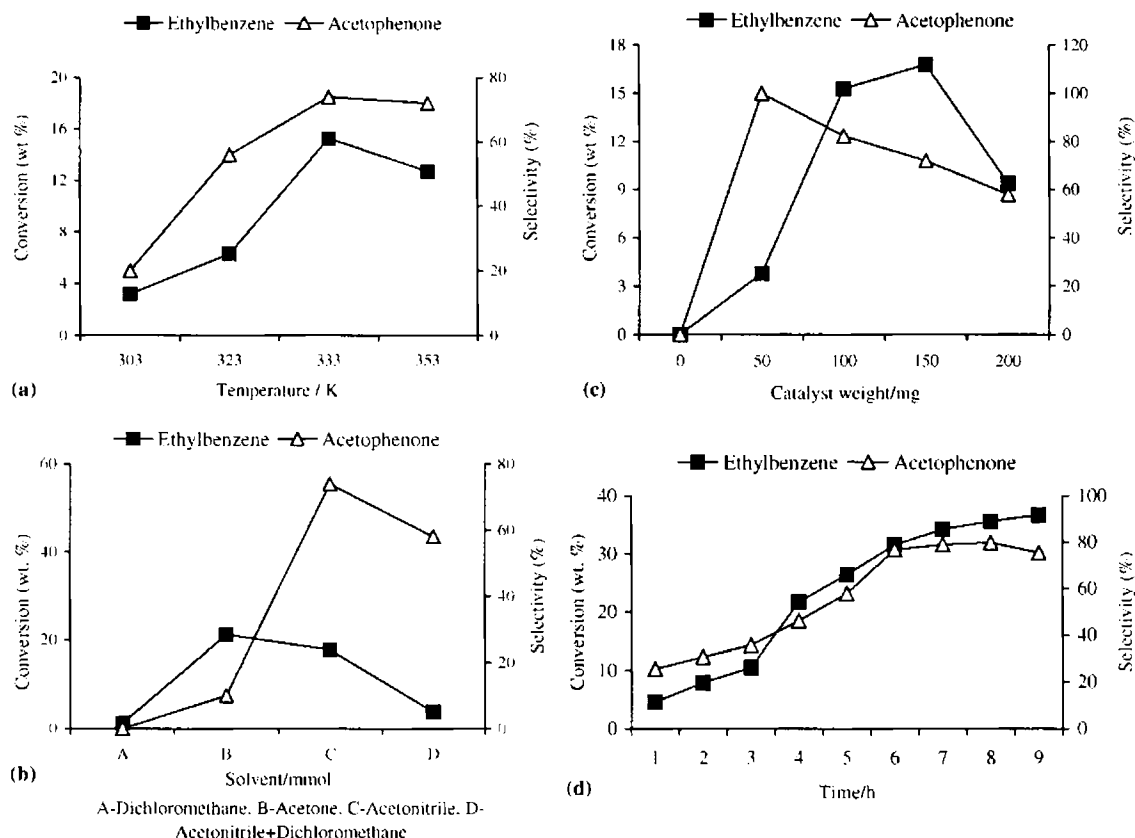

Fig. 4. Effect of reaction parameters on ethylbenzene oxidation: (a) reaction conditions: 6VC 100 mg, ethylbenzene - 8 mmol, acetonitrile - 95 mmol, H_2O_2 - 26 mmol and time - 3 h: (b) reaction conditions: 6VC - 100 mg, ethylbenzene - 8 mmol, solvent 95 mmol, H_2O_2 - 26 mmol, temperature - 333 K and time - 3 h: (c) reaction conditions: catalyst 6VC, ethylbenzene 8 mmol, acetonitrile 95 mmol, H_2O_2 - 26 mmol, temperature - 333 K and time - 3 h: (d) reaction conditions: 6VC - 100 mg, ethylbenzene - 8 mmol, acetonitrile 191 mmol, temperature - 333 K and H_2O_2 191 mmol.

333 K while further increase caused decrease in rate. Lower conversion rate at 353 K might be attributed to decomposition of H_2O_2 [34]. The selectivity to acetophenone increases as the temperature rises from 303 to 333 K and decreased at 353 K. This can result by further oxidation of acetophenone to hydroxy products. The influence of various solvents on oxidation is shown in Fig. 4(b). Generally, the role of solvent on the liquid-phase reaction is very complex, especially on the product distribution. Reaction conducted without any solvent and with dichloromethane did not produce any oxidized products. When acetonitrile and dichloromethane were used in 1:1 mole ratio, conversion and selectivity increased. Acetonitrile as solvent gave acetophenone selectively in high conversion rate. Acetonitrile being an aprotic solvent initiate side-chain oxidation at the interface with high conversion rate is known to activate H_2O_2 by forming a perhydroxyl anion, which in turn produces a good oxygen transfer intermediate [35,36]. Even though conversion is more in acetone, the acetophenone selectivity was very small. This can arise from side reactions between acidic solvent and H_2O_2 yielding peroxy or hydroperoxy products, causing a lower concentration of free H_2O_2 at or near the active sites [37]. The effect of catalyst amount on oxidation is presented in Fig. 4(c). The oxidation reaction was not observed in the absence of any catalyst indicating that H_2O_2 alone is unable to oxidize the substrate to a significant extent and reaction can occur only when a catalyst is present. It can be seen from the figure that the ethylbenzene conversion rate improves as the catalyst amount is increased reaches a maximum at 150 mg. Further increase to 200 mg decreases the conversion rate. High metal concentration can inhibit the autooxidation reactions [38]. However, acetophenone selectivity displays a different pattern. With 50 mg 6VC catalyst, acetophenone was produced as the main product while selectivity drops greatly as the catalyst amount increases to 200 mg. At lower catalyst concentration acetophenone was obtained as major product while at higher catalyst amount selectivity decreases at the cost of hydroxyacetophenone [39]. The effect of time on ethylbenzene oxidation is illustrated in Fig. 4(d). Acetophenone was the main product with lesser concentration of benzaldehyde and 2-hydroxyacetophenone. Conversion rate and selective formation of acetophenone increase with time up to 6 h. After 7 h of reaction conversion rate remains more or less constant while acetophenone selectivity decreases indicating further oxidation to form hydroxyl product under the reaction conditions. The polar oxidation and transformation products formed during reaction cover the surface of the solid oxide, can also lead to catalyst inactivation [40].

The studies on various reaction parameters show that oxidation rate and product selectivity in the liquid-phase oxidation of ethylbenzene is greatly dependent on a cooperative effect of the substrate, solvent, oxidant, time and temperature. The ethylbenzene oxidation reaction was carried out with all the catalysts prepared under the optimized reaction conditions and the results are shown in Table 2.

Table 2
Performance of catalysts in ethylbenzene oxidation

Catalyst	Conversion (wt%)	Selectivity (%)		
		Acetophenone	2-Hydroxy-acetophenone	Benzaldehyde
Ce	4.4	13.2	–	86.8
2VC	4.8	69.3	–	30.6
4VC	9.9	73.8		26.2
6VC	16.8	75.6	16.2	11.7
8VC	18.7	78.9	13.2	7.7
10VC	20.5	72.2	21.1	6.7

Reaction conditions: catalyst – 100 mg, ethylbenzene 8 mmol, acetonitrile 191 mmol, temperature 333 K, H_2O_2 – 26 mmol and time 6 h.

The oxidation reaction carried out over ceria has exhibited only negligible conversion with benzaldehyde as the major product. Supported vanadia catalysts were found to be active in the ethylbenzene oxidation with acetophenone as the major product. Benzaldehyde and 2-hydroxyacetophenone are also detected in minor quantities indicating that C–H bond activation takes place only at benzylic position. For a series of vanadia/ceria catalysts, activity increases with increase in loading up to 10 V_2O_5 wt% at which it gave a conversion of 20.5%. However, acetophenone selectivity decreases for 10VC with more amount of 2-hydroxyacetophenone.

Several mechanisms have been proposed for oxidation of ethylbenzene over redox catalysts. According to Singh et al. [41], the ethylbenzene oxidation over MeAPO-11 using TBHP involves an intermolecular mechanism, where the redox metal sites are catalytically active sites, which change its oxidation states after the reaction. They also observed that among the framework substituted McAPO-11s, VAPO-11 has maximum redox behaviour and is the most active with higher acetophenone selectivity. With vanadium silicates (VS-1 and VS-2) Ramaswamy et al. [42] proposed a peroxo radical intermediate capable of the side-chain oxidation in aromatic substrates. Ethylbenzene oxidation with Sn-Sil-1 is also reported through a peroxo radical ion intermediate giving acetophenone in major amount [43]. The studies of Reddy et al. [2] indicated that oxygen vacancies are the active sites and these vacancies are greatly influenced by geometric and electronic factors and are responsible for the formation of different products. Acetophenone and benzaldehyde are produced on terminal oxygen vacancy (M=O) sites while bridged oxygen vacancy sites are responsible for the formation of more oxygenated products. The side-chain oxidation of alkylbenzenes by cerium (IV) ammonium nitrate with bromate salt in acetic acid involves via an electron-transfer mechanism leading to the formation of radical cations as reaction intermediates. In the presence of cerium (IV) ammonium nitrate, where the Ce (IV) and bromate salts acts as efficient oxidants, the bromate salts act as a reoxidant for the Ce(III) ion. This reports that the Ce (IV) salts are catalysts for selective oxidation of alkylbenzenes [44]. The catalytic

redox cycle on ceria supported vanadia may be due to the redox cycle of cerium near vanadium; unlike the most supported vanadia catalysts, which work on the redox cycle of vanadium sites in accordance with a report for ceria supported chromia catalysts [45].

In the present study, vanadia/ceria catalysts were found active towards oxidation of ethylbenzene in liquid-phase. The observation shows that as the vanadia loading increases to 10 wt% V_2O_5, catalytic activity increases while acetophenone selectivity decreases. Benzaldehyde was also produced over these catalysts. When vanadia loading is higher above 6 wt% V_2O_5 it could oxidize the acetophenone formed to 2-hydroxyacetophenone as observed by the product analysis. Oxidation activity of vanadia/ceria catalysts could be correlated to the amount of the vanadia loaded and the structure of the species. The structural characterization of supported catalysts by XRD and FT-IR show the presence of highly dispersed vanadia on lower loading and formation of $CeVO_4$ as the vanadia loading increases to 10 wt% V_2O_5. Lower loading consists vanadia as tetrahedral V=O species while higher loading can lead to formation of Ce–O–V species on the support surface. ^{51}V MASNMR studies suggest the formation of $CeVO_4$ even with 6 wt% V_2O_5 on ceria and it increases with vanadia loading to 10 wt% V_2O_5. Aromatic ring hydroxylation was not observed when the reactions were carried using the prepared catalysts at the set conditions. Abstraction of alcoholic OH hydrogen and the CH hydrogen by the active oxygen yields acetophenone while similar abstraction of OH hydrogen of 1-phenylethanol by the active oxygen forms benzaldehyde. The oxidation activity associated with lower loaded VC catalysts attributed to the presence of highly dispersed tetrahedral V=O species on the support surface. Production of benzaldehyde is related to the presence of Ce–O–Ce and the V–O–V structure is related to the formation of acetophenone for these VC catalysts. The $CeVO_4$ formation observed with higher vanadia loading causes the oxidation of acetophenone to 2-hydroxyacetophenone.

4. Conclusions

The various supported vanadia catalysts exhibit efficient catalytic activity in the selective oxidation of ethylbenzene using H_2O_2. The oxidation with ceria supported vanadia catalysts afforded acetophenone as the main product. The VC series of catalysts exhibit enhanced activity and selectivity in the oxidation reaction. A direct relationship between the structural characteristics and oxidation behaviour is observed. Highly dispersed tetrahedral vanadia species evidenced by various spectroscopic techniques are selective for acetophenone production and Ce–O–V structure is related to the formation of 2-hydroxyacetophenone. The type of the active centers formed on the support catalysts determines the activity and product selectivity for the so prepared VC catalysts.

References

[1] X. Gao, I.E. Wachs, J. Catal. 192 (2000) 18.
[2] E.P. Reddy, R.S. Varma, J. Catal. 221 (2004) 93.
[3] S. Sugunan, N.K. Renuka, Bull. Chem. Soc. Jpn. 75 (2002) 463.
[4] V.P. Vislovskiy, J.S. Chang, M.S. Park, S.E. Park, Catal. Commun. 3 (2002) 227.
[5] K.V.R. Chary, G. Kishan, C.P. Kumar, G.V. Sagar, Appl. Catal. A 246 (2003) 335.
[6] H. Chen, A. Aleksandrov, Y. Chen, S. Zha, M. Liu, T.M. Orlando, J. Phys. Chem. B 109 (2005) 11257.
[7] S. Shylesh, T. Radhika, K. Sreejarani, S. Sugunan, J. Mol. Catal. A 236 (2005) 253.
[8] T. Radhika, S. Sugunan, J. Mol. Catal. A 250 (2006) 169.
[9] J.M. Vohs, T. Feng, G.S. Wong, Catal. Today 85 (2003) 303.
[10] M.M. Mohamed, S.M.A. Katib, Appl. Catal. A 287 (2005) 236.
[11] S.E. Dapurkar, A. Sakthivel, P. Selvam, New J. Chem. 27 (2003) 1184.
[12] G.L. Tembe, P.A. Ganeshpure, S. Satish, J. Mol. Catal. A 121 (1997) 17.
[13] R. Alcantara, L. Canoira, P.G. Joao, J.M. Santos, I. Vazquez, Appl. Catal. A 203 (2000) 259.
[14] N.K. Mal, V. Ramaswamy, S. Ganapathy, A.V. Ramaswamy, Appl. Catal. A 125 (1995) 233.
[15] K.O. Xavier, J. Chako, K.K.M. Yusuff, Appl. Catal. A 258 (2004) 251.
[16] P. Kumar, R. Kumar, B. Pandey, Synlett (1995) 289.
[17] F. Zhang, S.W. Chan, J.E. Spanier, E. Apak, Q. Jin, Appl. Phys. Lett. 80 (2002) 127.
[18] J.C. Badot, A. Mantoux, N. Baffier, O. Dubrunfaut, D. Lincot, J. Mater. Chem. 14 (2004) 3411.
[19] B.M. Reddy, P. Lakshmanan, A. Khan, J. Phys. Chem. 108 (4) (2004) 16855.
[20] G.S. Wong, J.M. Vohs, Surf. Sci. 498 (2002) 266.
[21] G.S. Wong, M.R. Concepcion, J.M. Vohs, J. Phys. Chem. B 106 (2002) 6451.
[22] J. Matta, D. Courcot, E. Abi-Aad, A. Aboukais, Chem. Mater. (2002) 4118.
[23] G.C. Bond, S.F. Tahir, Appl. Catal. 71 (1991) 1.
[24] M.V.M. Huerta, J.M. Coronado, M.F. Garcia, A.I. Juez, G. Deo, J.L.G. Fierro, M.A. Banares, J. Catal. A 225 (2004) 240.
[25] J. Matta, D. Courcot, E. Abi-Aad, A. Aboukais, J. Therm. Anal. Calorim. 66 (2001) 717.
[26] N.C. Wu, E.W. Shi, Y.Q. Zheng, W.J. Li, J. Am. Ceram. Soc. (2002) 2462.
[27] K. Mori, A. Miyamoto, Y. Murakami, J. Chem. Soc., Faraday Trans. 1 (83) (1987) 3303.
[28] J.R. Sohn, I.J. Doh, Y.I. Pae, Langmuir 18 (2002) 6280.
[29] M. Kantcheva, Phys. Chem. Chem. Phys. 2 (2000) 3043.
[30] H.E. Rast, H.H. Caspers, S.A. Miller, Phys. Rev. 169 (1968) 705.
[31] E.H. Park, M.H. Lee, J.R. Sohn, Bull. Korean Chem. Soc. 21 (2000).
[32] B. Olthof, A. Khodakov, A.T. Bell, E. Inglesia, J. Phys. Chem. B 104 (2000) 1516.
[33] R. Cousin, D. Courcot, E. Abi-Aad, S. Capelle, J.P. Amoureux, M. Dourdin, A. Aboukais, Colloid Surf. A 158 (1999) 43.
[34] R. Yu, F. Xiao, D. Wang, T. Sun, Y. Liu, G. Pang, S. Feng, S. Qui, R. Xu, C. Fang, Catal. Today 51 (1999) 39.
[35] U.R. Pillai, E.S. Demessie, J. Mol. Catal. A 191 (2003) 93.
[36] S. Shylesh, A.P. Singh, J. Catal. 228 (2004) 333.
[37] U. Wilkenhoner, G. Langhendries, F. van Laar, G.V. Baron, D. Gammon, P.A. Jacobs, E. van Steen, J. Catal. 203 (2001) 201.
[38] L.C.W. Baker, V.W. Simons, J. Am. Chem. Soc. 81 (1959) 4744.
[39] J.M. Thomas, R. Raja, Chem. Commun. (2001) 675.
[40] O.T. Kasaikina, V.D. Kortenska, Z.S. Kartasheva, G.M. Kuznetsova, T.V. Maximova, T.V. Sirota, N.V. Yanishlieva, Colloid Surf. – Physicochem. Eng. Aspects 149 (1999) 29.

[41] P.S. Singh, K. Kosuge, V. Ramaswamy, B.S. Rao, Appl. Catal. A 177 (1999) 149.
[42] P.R.H.P. Rao, A.V. Ramaswamy, J. Chem. Soc., Chem. Commun. (1992) 1245.

[43] N.K. Mal, A.V. Ramaswamy, Appl. Catal. A 143 (1996) 75.
[44] E. Ganin, I. Amer, J. Mol. Catal. A 116 (1997) 323.
[45] J.E. Remias, T.A. Pavlosky, A. Sen, J. Mol. Catal. A 203 (2003) 179.